

Effect of Radiation Dose on the Thermal Degradation of Poly(ethylene terephthalate) Fabric

E. H. El-Gendy,¹ I. A. El-Shanshoury²

¹National Center for Radiation Research and Technology, Atomic Energy Authority, P.O. Box 29, Nasr City, Cairo 11731, Egypt

²National Center for Nuclear Safety and Radiation Control, Atomic Energy Authority, P.O. Box 29, Nasr City, Cairo 11731, Egypt

Received 2 May 2003; accepted 1 December 2003

ABSTRACT: The effect of radiation dose (10–30 kGy) on the thermal decomposition of poly(ethylene terephthalate) was studied using thermogravimetric analysis (TGA), differential scanning calorimetry (DSC), and X-ray diffraction (XRD) analysis. The TGA and DSC were carried out in a flowing nitrogen atmosphere at heating rates of 5 and 30°C/min for TGA and 10°C/min for DSC. The degradation process was composed of three overlapping stages. The second stage, at which a rapid degradation occurs, was studied in detail. The process was found to follow a second-order kinetics and was independent of radiation dose or heating rate. The reaction rate constant (k) was found to depend on the heating rate and irradiation dose. The apparent activation energy (Q) and the logarithm of the preexponential rate constant ($\log A$) were found to decrease linearly with the increase in dose at rates of $3.32 \text{ kJ mol}^{-1} \text{ kGy}^{-1}$ and $0.177 \text{ s}^{-1} \text{ kGy}^{-1}$ with intercepts of 249 kJ/mol and 12.26 s^{-1} for Q and $\log A$ of unirradiated fabric, respectively. A direct relationship was found between the percentage decrease in Q and $\log A$ and the percentage decrease in the temperature

corresponding to 50% conversion ($T_{50\%}$) for samples irradiated at different doses. It was found that a decrease in $T_{50\%}$ by 1% resulted in a decrease in Q and $\log A$ by 1.855 and 2.1%, respectively. Changes in Q and $\log A$ resulting from radiation, mechanical and thermal treatments, or their combinations can be predicted from the shift in $T_{50\%}$. The history of the fibers substantially affected the thermal properties. DSC and XRD studies revealed changes in the fabric crystallinity. DSC measurements indicated a linear increase in heat of fusion with dose increase at a rate of $0.855 \text{ kJ kg}^{-1} \text{ kGy}^{-1}$. XRD analysis confirmed structural changes, rearrangement by plane rotations, and formation of compact crystalline lattice with patterns characterizing irradiated samples. An attempt to explain the dependency of the apparent activation energy on dose was given. © 2004 Wiley Periodicals, Inc. *J Appl Polym Sci* 92: 3710–3720, 2004

Key words: radiation; thermogravimetric analysis (TGA); poly(ethylene terephthalate) (PET); kinetics (polym.); X-ray

INTRODUCTION

In 1996, 24.1 million metric tons of man-made fibers were produced worldwide. The main volume gain took place in production of poly(ethylene terephthalate) (PET) fibers.¹ The primary drive for this growth is demand for fiber and resin for containers. Seventy-five percent of the entire PET production is directed toward the manufacture of fiber. Dramatic growth in PET fiber production is foreseen in Asia in the near future.²

The cost of polyester, with its combination of superior strength and resilience, is lower than that of rayon. Polyester fibers are hydrophobic, which is desired for lightweight facing fabrics used in the disposal industry.

Polyester fiber is a manufactured fiber in which the fiber-forming substance is any long-chain synthetic

polymer composed at least of 85% by weight of an ester of dihydric alcohol (HOROH) and terephthalic acid ($p\text{-HOOC-C}_6\text{H}_4\text{COOH}$). The most widely used polyester fiber is made from the linear polymer PET. High strength, high modulus, low shrinkage, heat set stability, light fastness, and chemical resistance account for the great versatility of PET.

Because of its rigid structure, well-developed crystallinity, good thermal properties, high hydrophobic properties, and lack of reactive dye sites, PET requires modification of its properties. Modification of the properties of PET fiber is usually carried out by radiation grafting with ionizing radiation. Modifications of the swelling properties and the dyeability of PET fabric toward reactive and basic dyes, using gamma radiation grafting, were studied in our previous investigations.^{3,4} Electron beam radiation grafting of PET, cotton, and PET–cotton blends, with special monomers, were studied by Stannett et al.,⁵ Liepins et al.,⁶ and Zahran et al.⁷ to impart flame resistance and flame proofing, and to overcome the drawbacks in its thermal properties, given that PET is flammable and the fabric usually melts and drops away instead of

Correspondence to: E. El-Gendy (eglal_elgendy@hotmail.com).

spreading. PET fiber will burn and cotton blending supports combustion. Similar investigations on grafting flame retardants onto PET/cotton blends by electron beam-induced grafting were reported by Choi et al.,⁸ Kong et al.,⁹ and Kaji et al.¹⁰ Nor¹¹ reported that differential scanning calorimetry (DSC) measurements showed that the melting temperature of grafted PET fibers decreases slightly as the percentage of grafting increases.

It is quite clear that in all radiation grafting experiments the backbone of PET fibers will be exposed to radiation effects, which results in changes in the thermal properties of the material. Consequently, this article reports studies on the effect of gamma radiation dose on the thermal stability of unirradiated PET fabrics, based on the experimental results of thermogravimetric analysis (TGA), DSC, and X-ray diffraction analysis (XRD). The effects of radiation dose on the structure of the fabric as well as on the reaction order, the reaction rate constants, the preexponential rate constant, and the apparent activation energy for thermal degradation and/or decomposition were studied using the mentioned methods. Coupling of the thermodynamic and structural characteristics of PET with its properties for practical use (e.g., mechanical properties, physicochemical properties, etc.) are given.

THEORY

The TGA method is widely used to investigate the thermal stability of polymers by determination of the decomposition or degradation kinetics, such as the reaction order (n), the conversion rate constant (R_C), and the activation energy (Q).

The rate of thermal decomposition of polymers is generally expressed as

$$dC/dt = k_C(1 - C)^n \quad (1)$$

where dC/dt (R_C), C , k_C , and n are the rate of conversion (fraction converted per time), the conversion, the reaction rate constant, and the reaction order, respectively. The weight remaining ($1 - C$) is expressed as a fraction in this work. The rate constant k_C is temperature dependent and follows the Arrhenius rate equation

$$k_C = Ae^{-Q/RT} \quad (2)$$

where A , Q , R , and T are the preexponential rate factor, the activation energy, the universal gas constant, and the absolute temperature, respectively. If the heating rate dT/dt of the sample is defined as β , then eq. (1) can be rewritten as

$$dC/dt = \beta(dC/dT) = k(1 - C)^n \quad (3)$$

The rate of conversion is determined from eq. (3) by computing the value of the change in conversion by the change in the absolute temperature (the slope dC/dT) at a constant conversion and multiply by the heating rate β . The reaction order n can thus be calculated by rearranging eq. (3) by taking logarithm of both sides, such that

$$\log(dC/dt) = \log k_C + n \log(1 - C) \quad (4)$$

Because the values of C and $(1 - C)$ are fractions and the rate of conversion decreases with the increase in the fraction remaining, the values of the slope n and $\log k$ of the straight-line relationship between $\log R_C$ and $\log(1 - C)$ are negative in sign. Both values, n and $\log k_C$, are obtained from equations displayed on the computer chart.

The activation energy of decomposition and/or degradation process is calculated from the values of the rate constants by carrying out the experiment at two different heating rates, β_1 and β_2 . Based on the displacement of the thermogravimetric curve attributed to the increase of heating rate, several methods have been used to calculate the value of Q . By comparing two thermograms with different heating rates, it can be deduced from eq. (2) that

$$k_{C1}/k_{C2} = e^{-(Q/R)[(1/T_1)-(1/T_2)]}$$

where T_1 and T_2 are the absolute temperatures at the same degree of conversion for heating rates β_1 and β_2 , respectively. By taking the natural logarithm of both sides, one obtains

$$\ln(k_{C1}/k_{C2}) = -Q/R[(1/T_1) - (1/T_2)]$$

By rearranging and inserting the values of the universal gas constant (R) and the factor to change $\ln(x)$ to $\log(x)$, then one obtains

$$Q \text{ (J/mol)} = 19.04T_1T_2(T_2 - T_1)^{-1}\log(k_2/k_1) \quad (5)$$

The value of $\log(k_{C2}/k_{C1})$ is obtained from the difference between the logarithms of k_{C2} and k_{C1} displayed on the chart as given previously.

In most of the experiments the rate of conversion was maximum between 40 and 50% conversion. The temperatures corresponding to 50% conversion ($T_{50\%}$) are usually taken to calculate Q , although other temperatures corresponding to constant conversion between 10 and 50% can be used as well. Deviations in the value of Q were observed at 10 and 20% conversions.

The value of the preexponential rate constant A was calculated from eq. (2) by taking the natural logarithm of both sides and rearranging, as follows:

$$\log A \text{ (s}^{-1}\text{)} = \log k_C \text{ (s}^{-1}\text{)} + Q/(2.3RT) \quad (6)$$

The value of $\log A$ was calculated by inserting the proper values of Q , R , and $\log k_C$ at the corresponding values of $T_{50\%}$ and heating rate.

The above given mathematical approach avoids consideration of the equality of the slopes $(dC/dT)_1$ and $(dC/dT)_2$ at the corresponding heating rates as well as the tedious method for calculating the reaction order as given by Sundardi et al.¹² Moreover, eq. (5) is more accurate than that given by Ozawa^{13,14} in calculating Q because the reaction order is included in the value of $\log k_C$, in that it equals $\log \beta(dC/dT) + n \log(1 - C)$. In Ozawa's work, the value of $\ln(\beta_2/\beta_1)$ was used rather than the values of the rate constants, based on the assumption of parallel slopes of the thermograms at different heating rates. Reich¹⁵ introduced the $(T_1/T_2)^2$ term in Ozawa's equation as a correction factor. Based on the experimental results, there are significant differences in the values of n calculated in this work and those reported by Sundardi et al. The calculated Q values are reasonably close to those given by Ozawa and Reich.

EXPERIMENTAL

Materials and methods

Thermally stabilized (heat treated at 493 K for 1.5 min) low-density polyester (PET) fabric, a product of Hankook Synthetic Inc. (Korea), was mill-scoured in a solution containing 0.001 g/L Data scour WS-100 and sodium carbonate (0.5 g/L) at boil for 1 h. The fabric was thoroughly washed with hot water, dried at ambient temperature, and then used for irradiation.

The PET fabric was irradiated in a ⁶⁰Co gamma source of 1.98 Gy/s dose rate for 10, 20, and 30 kGy doses. Irradiation was conducted under nitrogen atmosphere.

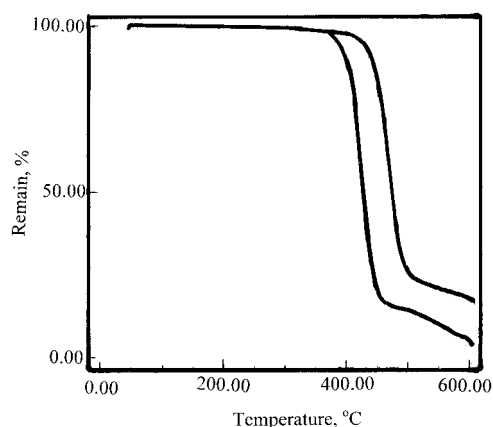


Figure 1 TGA curves for unirradiated PET samples heated in nitrogen at heating rates of 5 and 30°C/min.

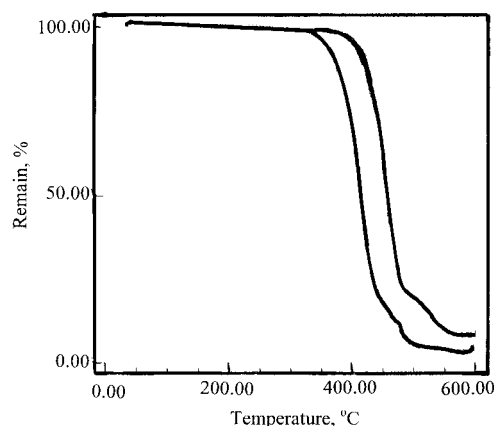


Figure 2 TGA curves for PET samples irradiated to 30 kGy and heated at rates of 5 and 30°C/min.

Apparatus

TGA studies were carried out on a Shimadzu TGA-30 apparatus (Shimadzu, Kyoto, Japan) at heating rates of 5 and 30°C/min in a nitrogen atmosphere over a temperature range from room temperature to 873 K. The primary TGA thermograms were used to determine the effect of different treatments on the thermal stability of PET samples. The primary thermograms conducted at 5 and 30°C/min heating rates were used to determine different kinetic parameters.

The degree of conversion and percentage remaining of the sample were calculated as follows:

$$\text{Degree of conversion (\%)} = 100[(W_0 - W_T)/W_0] \quad (7)$$

$$\text{Remainder of sample (\%)} = 100(W_T/W_0) \quad (8)$$

where W_0 and W_T are the weights of the original and heated samples, respectively. The weight fractions converted C or remained $(1 - C)$ are the same as given in eqs. (7) and (8) without percent.

DSC studies were performed using a Perkin-Elmer DSC-7 calorimeter (Perkin Elmer Cetus Instruments, Norwalk, CT). A heating rate of 10°C/min was used under a nitrogen atmosphere.

X-ray diffraction analysis (XRD) was performed using a Shimadzu DP-DI with Cu-K α characteristic radiation.

RESULTS AND DISCUSSION

Thermogravimetric analysis

Representative TGA thermograms for unirradiated and irradiated (30 kGy) PET fabric are given in Figures 1 and 2, respectively, for the nominal heating rates of 5 and 30°C/min. The general features of the percentage remaining weights as a function of temperature are the same except that the curves shift to the right

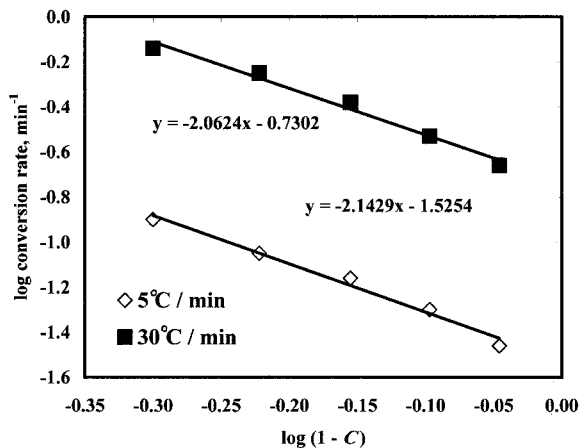


Figure 3 Logarithmic plots of conversion rate versus weight fraction remaining for unirradiated samples.

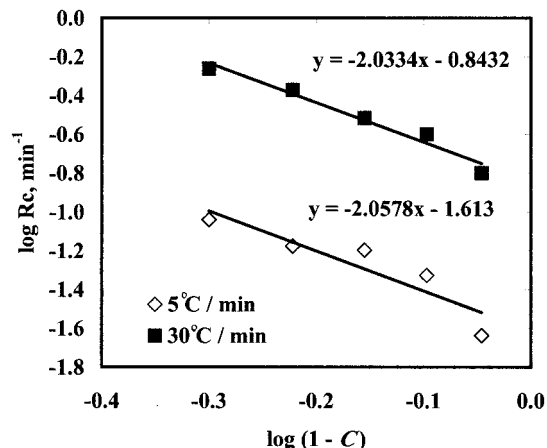


Figure 5 Logarithmic plots of conversion rate versus weight fraction remaining for samples irradiated to 20 kGy dose.

(higher temperature) as the heating rate increases. The thermograms show three overlapping degradation processes. The first process occurs from room temperature to about 400°C, depending on the heating rate and irradiation condition, and is a very slow degradation process. The second process is extremely fast, with transitions above 400°C, and occurs within 0.1–0.8 weight fraction converted. The third stage takes place around 0.86 and 0.92 fraction converted, after which complete decomposition of the fabric occurs. This study is mainly concerned with the second stage at the temperature range where the fast fabric degradation or decomposition takes place.

The values of the rates of conversion (dC/dt) were calculated from the thermograms by multiplying the value of dC/dT , the slope of the fraction weight remaining, and the temperature at a constant conversion (fraction), by the value of the corresponding heating rate. The logarithm of the rate of conversion [$\log(dC/dt)$] is then plotted as a function of the logarithm of fraction remaining [$\log(1 - C)$], according to eq. (4). Figures 3–6 show the linear relationship between the logarithm of rate of conversion R_C (fraction converted/min) and the logarithm of the fraction remaining $(1 - C)$ for PET fabric irradiated at doses (D) ranging from zero, for unirradiated, to 30 kGy and heated at rates of 5 and 30°C/min. The equations relating the conversion rate R_C , the reaction order n , and the reaction rate constant k_C are as follows:

For unirradiated PET

$$(\log R_C)_{5^\circ\text{C}/\text{min}} = -2.1429 \log(1 - C) - 1.5240 \quad (9)$$

$$(\log R_C)_{30^\circ\text{C}/\text{min}} = -2.0624 \log(1 - C) - 0.7302 \quad (10)$$

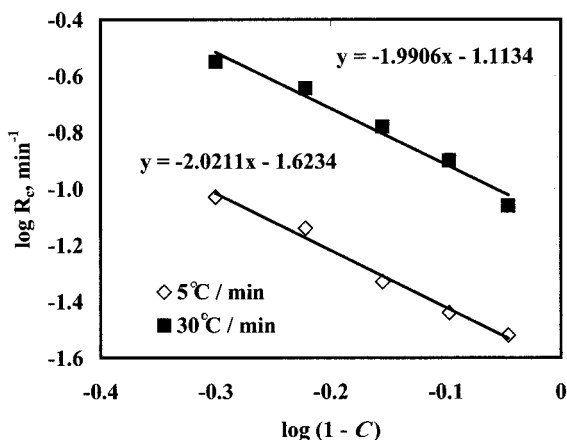


Figure 4 Logarithmic plots of conversion rate versus weight fraction remaining for samples irradiated to 10 kGy dose.

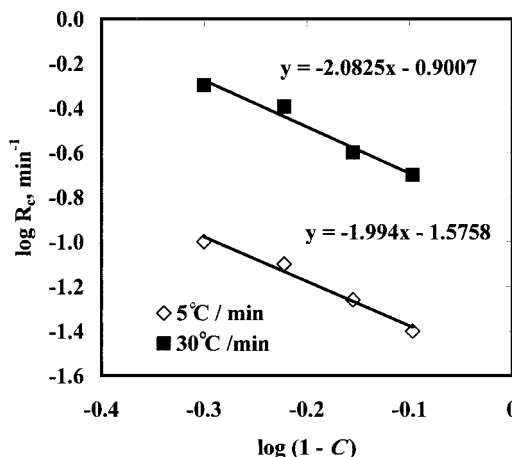


Figure 6 Logarithmic plots of conversion rate versus weight fraction remaining for samples irradiated to 30 kGy dose.

TABLE I
Effect of Radiation Dose on the Reaction Order (n), the Rate Constant (k_c), the Activation Energy (Q), and the Preexponential Rate Constant (A) of PET Fabric

| Fiber | Reaction order (n) | $\log k_c$ at | | k_c (s^{-1}) at | | Q (kJ/mol) | $\log A$ (s^{-1}) |
|--------------|------------------------|---------------|----------|-----------------------|-----------------------|-------------------|-----------------------|
| | | 5°C/min | 30°C/min | 5°C/min | 30°C/min | | |
| Unirradiated | | | | | | | |
| PET | 2.1 (± 0.038) | -1.5254 | -0.7302 | 4.97×10^{-4} | 3.10×10^{-3} | 243 (± 9.6) | 12.08 |
| PET 10 kGy | 2.0 (± 0.004) | -1.6234 | -1.1134 | 3.97×10^{-4} | 1.28×10^{-3} | 227 (± 6.3) | 10.86 |
| PET 20 kGy | 2.08 (± 0.05) | -1.6210 | -0.8537 | 3.99×10^{-4} | 2.33×10^{-3} | 178 (± 5.1) | 8.54 |
| PET 30 kGy | 2.08 (± 0.004) | -1.5758 | -0.9007 | 4.43×10^{-4} | 2.10×10^{-3} | 149 (± 7.1) | 6.96 |

For 10 kGy dose

$$(\log R_C)_{5^\circ\text{C}/\text{min}} = -2.0211 \log(1 - C) - 1.6234 \quad (11)$$

$$(\log R_C)_{30^\circ\text{C}/\text{min}} = -1.9906 \log(1 - C) - 1.1134 \quad (12)$$

For 20 kGy dose

$$(\log R_C)_{5^\circ\text{C}/\text{min}} = -2.0836 \log(1 - C) - 1.6210 \quad (13)$$

$$(\log R_C)_{30^\circ\text{C}/\text{min}} = -2.0746 \log(1 - C) - 0.8537 \quad (14)$$

For 30 kGy dose

$$(\log R_C)_{5^\circ\text{C}/\text{min}} = -1.9940 \log(1 - C) - 1.5758 \quad (15)$$

$$(\log R_C)_{30^\circ\text{C}/\text{min}} = -2.0746 \log(1 - C) - 0.9007 \quad (16)$$

The slope of the linear relationship between $\log R_C$ and $\log(1 - C)$ gives the reaction order n . The sign of n is negative because the value of $\log R_C$ (min^{-1}) decreases with the increase in $\log(1 - C)$. The constant of the linear relationship gives the value of $\log k_C$ (min^{-1}). It is clear from the results that the values of

$\log k_C$ are negative and increase with the increase in the heating rate. Table I shows the values of n and $\log k_C$ at the corresponding heating rates. It also shows that the value of n is constant and independent of the irradiation dose or the heating rate and indicates a second-order kinetics.

The activation energy for the degradation process can be calculated from eq. (5) by inserting the proper values of $\log(k_{C2}/k_{C1})$ [i.e. $(\log k_{C2} - \log k_{C1})$], given in Table I, and the absolute temperatures T_1 and T_2 at 40 or 50% conversion for the 5 and 30°C/min heating rates, respectively. Table I also shows the values of the rate constants at the corresponding heating rate. The magnitude of k_c is in the order of 10^{-4} and $10^{-3} s^{-1}$ for the heating rates 5 and 30°C/min, respectively, and is dose dependent. The calculated values of the apparent activation energy are listed in Table I in kJ/mol.

The preexponential rate constant A is calculated from eq. (6). Its value, in $\log A$, is calculated from $\log k_C$, the activation energy Q , the universal gas constant R ($8.3136 \text{ J mol}^{-1} \text{ K}^{-1}$), and the absolute temperature ($T_{50\%}$) at the corresponding heating rate. The values of $\log A$ for PET fabric irradiated at different doses are listed in Table I.

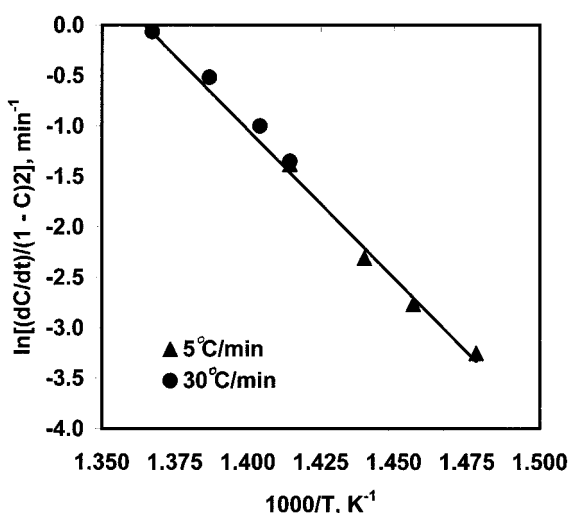


Figure 7 Arrhenius plot of the second reaction order of the thermal degradation of unirradiated PET fabric.

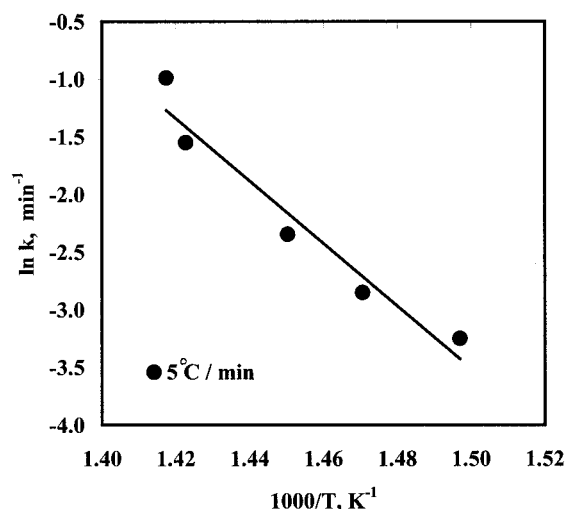


Figure 8 Arrhenius plot of the second reaction order of the thermal degradation of PET fabric, irradiated with a dose of 10 kGy.

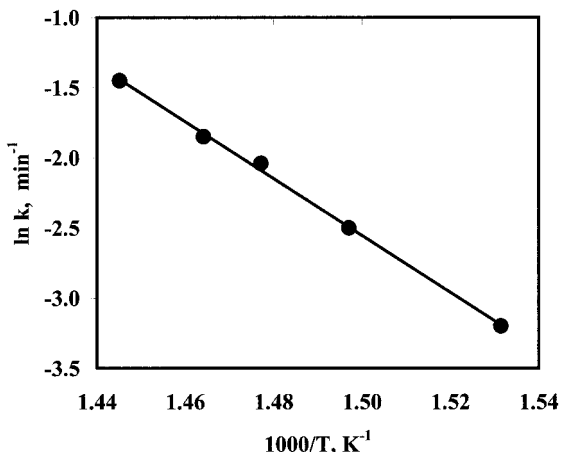


Figure 9 Arrhenius plot of the second reaction order of the thermal degradation of PET fabric, irradiated with a dose of 20 kGy.

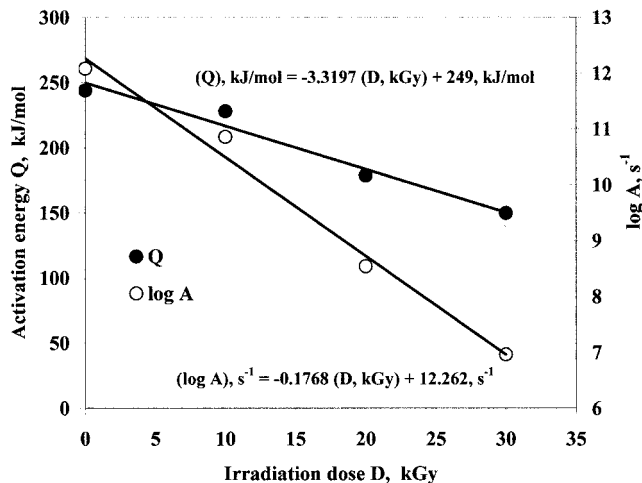


Figure 10 Dependency of the activation energy of thermal degradation (Q) and the natural logarithm of the preexponential rate constant ($\log A$) on radiation dose.

To confirm the second-order dependency of the decomposition process, the values of the natural logarithm of $[R_C/(1 - C)^2]$ (min⁻¹), $\ln k_C$, is plotted as a function of $1/T$ (K⁻¹) according to Arrhenius eq. (6). Figures 7–9 show linear dependency with activation energies of 244, 226, and 179 kJ/mol for unirradiated and 10 and 20 kGy doses, respectively. These values are similar to those given in Table I.

The results presented in Table I give different relations between the irradiation dose D and the activation energy as well as the logarithm of the preexponential rate constant ($\log A$). The values of Q and $\log A$ decrease with the increase in dose. The dependency of Q and $\log A$ on D is shown in Figure 10. The relationships show a linear decrease of both dependent variables with an increase in D , according to the following equations:

$$Q \text{ (kJ/mol)} = -3.32D \text{ (kGy)} + 249 \text{ (kJ/mol)} \quad (17)$$

$$\log A \text{ (s}^{-1}\text{)} = -0.177D \text{ (kGy)} + 12.26 \text{ (s}^{-1}\text{)} \quad (18)$$

Equations (17) and (18) indicate that the values of Q and $\log A$ decrease linearly with an increase in D at

3.32 kJ/mol and 0.177 s^{-1} as the irradiation dose increases by 1 kGy. The intercept of the straight lines with the y -axis at zero dose give values of 249 kJ/mol and 12.26 s^{-1} for Q and $\log A$, respectively, for the unirradiated PET fabric. These results are different from those reported by Sundardi et al.¹² (Table II). In their work, the authors showed that the reaction order increases from 1.3 to 1.5 for the unirradiated and irradiated to 20 kGy dose. With a further increase in dose (from 40 to 60 kGy) the reaction order decreased to 0.9 and then increased to 1.6. The activation energy values corresponding to the doses are 204, 207, 180, and 214 kJ/mol, respectively. However, their results show an increase in Q with the increase in dose, which completely contradicts our results (Fig. 10 and Table I).

The results of Figure 10 can logically be explained by the radiation degradation of the structure of PET fiber, which results in the decrease in the polymer molecular weight and consequently the activation energy for fiber decomposition. Moreover, our value for n is constant (second-order) and is independent of dose or heating rate, which indicates that the mecha-

TABLE II
Kinetic Parameters of Thermal Degradation of Irradiated PET Fabric: Comparative Study with Sundardi's Work

| Fiber | Sundardi et al. | | This work | |
|--------------|---------------------|---------------------------------|---------------------|---------------------------------|
| | Reaction order, n | Activation energy, Q (kJ/mol) | Reaction order, n | Activation energy, Q (kJ/mol) |
| PET (0 kGy) | 1.3 | 204 | 2.1 | 243 |
| PET (10 kGy) | | | 2.0 | 227 |
| PET (20 kGy) | 1.5 | 207 | 2.05 | 187 |
| PET (30 kGy) | | | 2.1 | 149 |
| PET (40 kGy) | 0.9 | 180 | | |
| PET (60 kGy) | 1.6 | 214 | | |

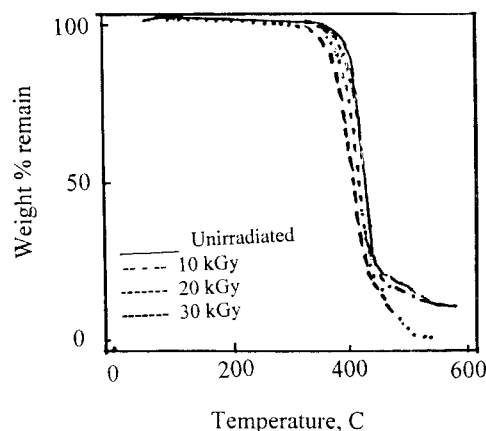


Figure 11 Effect of radiation dose on the TGA thermogram of PET fabric, heated at 5°C/min.

nism of degradation in the used doses and weight fractions is almost the same. Extrapolating the dependency of Q on n , in the work of Sundardi et al., to $n = 2$ gives an activation energy of about 234 kJ/mol, which is close to the results of this work.

Irradiation of PET fiber shifts the TGA thermograms to lower temperatures. Figure 11 shows the decrease in the range of all temperatures above 673 K up to the complete decomposition with the increase of dose for samples heated at 5°C/min. There was no significant effect of the dose on the degradation of PET fabric up to about 598 K. The temperature corresponding to 50% conversion ($T_{50\%}$) is considered as a measure of the thermal stability of the fabric because the rate of conversion at $T_{50\%}$ is maximum. The value of $T_{50\%}$ decreases linearly from 698 to 677 K as the irradiation dose increases to 30 kGy (Fig. 12). The equation governing this relationship is as follows:

$$T_{50\%} \text{ (K)} = -0.7D \text{ (kGy)} + 698 \text{ (K)} \quad (19)$$

The value of the slope of the relationship indicates that increasing the dose by 1 kGy decreases $T_{50\%}$ by 0.7 K. The intercept gives the value of $T_{50\%}$ of the unirradiated PET fabric (698 K). Figure 12 also shows the dependency of the activation energy on the dose according to eq. (17). Grouping Figures 10 and 12 results in a relationship relating both Q and $\log A$ to $T_{50\%}$. Figure 13 shows that the percentage decrease in Q and $\log A$, attributed to irradiation, increases linearly with the percentage decrease in $T_{50\%}$ (°C). The relationships are expressed in the following equations:

$$\Delta Q/Q \text{ (\%)} = 1.855(\Delta T_{50\%}/T_{50\%}) \text{ (\%)} \quad (20)$$

$$\Delta \log A/\log A \text{ (\%)} = 2.1(\Delta T_{50\%}/T_{50\%}) \text{ (\%)} \quad (21)$$

These equations show that a decrease in $T_{50\%}$ by 1% results in a decrease in Q and $\log A$ by 1.855 and 2.1%,

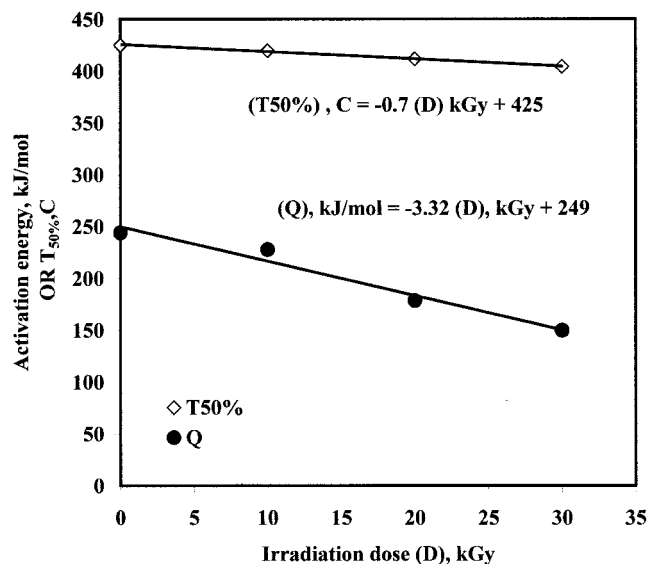


Figure 12 Relationship between the activation energy Q and the temperature corresponding to 50% conversion ($T_{50\%}$) at different radiation doses.

respectively. The relationships relating the changes in both Q and $\log A$ with the change in $T_{50\%}$, attributed to irradiation, are extremely important and can be generalized to any external source that causes fiber degradation. Changes in Q and $\log A$ resulting from radiation, mechanical or thermal treatments, or combinations of different treatments that cause a decrease in $T_{50\%}$ can be predicted directly from eqs. (20) and (21) by measuring the shift in $T_{50\%}$. Consequently, it can be emphasized that the history of the fabric substantially affects its thermal properties.

The effect of D on the thermal stability of the fabric, as measured by the degree of conversion, is clarified

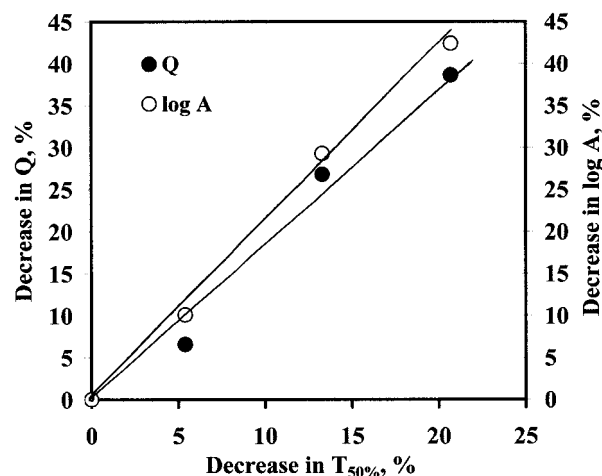


Figure 13 Dependency of the percentage decrease in Q and $\log A$ on the percentage decrease in $T_{50\%}$ for samples irradiated at different doses.

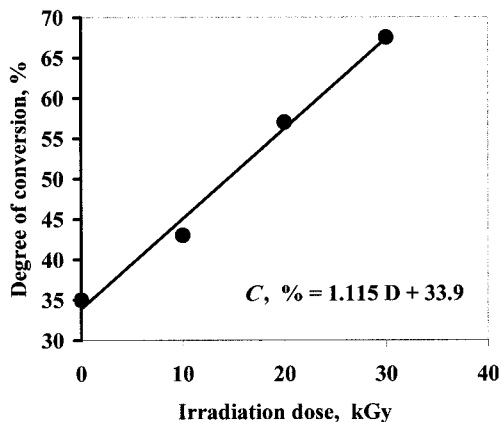


Figure 14 Dependency of the degree of conversion on radiation dose for PET samples, measured at 415°C at a heating rate of 5°C/min.

by measuring the weight percentage of fabric converted or degraded at 688 K (midvalue of $T_{50\%}$). Figure 14 shows that the degree of conversion increases linearly with the increase of D according to the relationship

$$\text{Conversion (\%)} = 1.12D + 33.9\% \quad (22)$$

Equation (22) indicates that the value of the degree of conversion of unirradiated PET fabric, measured at 688 K, is 33.9%. An increase in dose by 1 kGy increases the degree of conversion by 1.12%.

Comparison of the results of this work for Q and $\log A$ for the unirradiated PET fiber with those reported in the literature for the second stage of the degradation process is shown in Table III. Table III shows that the values of the reaction order n , the activation energy Q , and $\log A$, given in this work, are similar to those obtained from the method of Friedman¹⁶ and Freeman–Carroll¹⁷ for n , Chatterjee–Conrad¹⁸ and Freeman–Carroll¹⁷ for Q , and Ozawa¹³ for $\log A$. Moreover, comparison of the value of Q (Table III) with those reported by Cooney et al.¹⁹ (191.8 kJ/mol), Gooding,²⁰ Birdladeanu et al.²¹ (249 and 272 kJ/mol in air and N_2 , respectively), Hedges et al.²² (292 kJ/mol), Matusевич and Kumachev²³ (up to 243 kJ/mol in air), and Bechev et al.²⁴ (up to 333 kJ/mol) indicates that the activation energy calculated in this work falls within the values reported by these investigators. The high value of the activation energy calculated from our method is attributed to heating the samples in nitrogen atmosphere. Thermograms carried out in air yield activation energies lower than those obtained in nitrogen because decomposition of the fiber in air is enhanced by the oxidation process.

Differential scanning calorimetry

The values of glass-transition temperature T_g , melting temperature T_m , and the corresponding values of the

TABLE III Comparison of the Kinetic Data for the Second Stage of Thermal Degradation of Unirradiated PET Fiber Given in This Work and That of Cooney et al. According to the Methods Given by Different Authors

| Variable | Kissinger ²⁵ | Freeman–Carroll ¹⁷ | Chatterjee–Conrad ¹⁸ | Friedman ¹⁶ | Horowitz–Metzger ²⁶ | Coats–Redfern ²⁷ | Ozawa ¹³ | Sundardi et al. ¹² | This work |
|--|-------------------------|-------------------------------|---------------------------------|------------------------|--------------------------------|-----------------------------|---------------------|-------------------------------|--------------|
| Fractional weight loss | 0.36–0.92 | 0.17–0.74 | 0.05–0.40 | 0.35–0.8 | 0.1–0.8 | 0.14–0.66 | 0.5 | — | 0.1–0.5 |
| Heating rate (°C/min) | 0.1 | 5 | 10 | — | 5 | — | — | 5–30 | 5–30 |
| Order of reaction, n | 1.0 | 1.7 ± 0.4 | 1.0 | 2.0 ± 0.02 | 1.0 | 1.5 | — | 1.3 | 2.07 |
| Activation energy, Q (kJ/mol) | 202 ± 6.7 | 293 ± 48.3 | 241 ± 7.5 | 201 ± 8.5 | 199 ± 5.1 | 218 ± 4.8 | 182 ± 7.4 | 204 ± 6.77 | 243.86 ± 9.6 |
| $\log A$ (s ⁻¹) ^a | — | — | — | 6.82 ± 0.2 | — | — | 12.7 ± 0.34 | — | 12.08 ± 0.3 |

^a All values of $\log A$ have been calculated to s⁻¹ rather than min⁻¹.

TABLE IV
Effect of Different Treatments on the Thermal Properties of PET Fabric Obtained from DSC Analysis

| Treatment | T_g (°C) | T_m (°C) | ΔH_g (kJ/kg) | ΔH_f (kJ/kg) |
|--------------|------------|------------|----------------------|----------------------|
| Unirradiated | Undetected | 257 | Undetected | 31 |
| 10 kGy | Undetected | 259 | Undetected | 46 |
| 20 kGy | Undetected | 258 | Undetected | 51 |
| 30 kGy | 78 | 258 | Undetected | 58 |

energy required for the fusion of PET samples having different radiation treatments are shown in Table IV. Figure 15 gives examples of DSC thermograms for unirradiated samples heated at 10°C/min. It can be seen from Table IV that irradiating PET samples to 10, 20, and 30 kGy dose did not reveal the peaks at T_g with only a slight effect at 30 kGy dose ($T_g = 351$ K). The crystalline melting point and the heat of fusion are affected differently by irradiation. No observable radiation effect is noticed for T_m and its value is around 531 K. The heat of fusion (ΔH_f), however, was found to increase with the increase in dose. Its value increased from 31 to 58 kJ/kg as the dose increased from zero to 30 kGy. Figure 16 shows a linear dependency of ΔH_f on dose D , according to

$$\Delta H_f = 0.855D + 34 \quad (23)$$

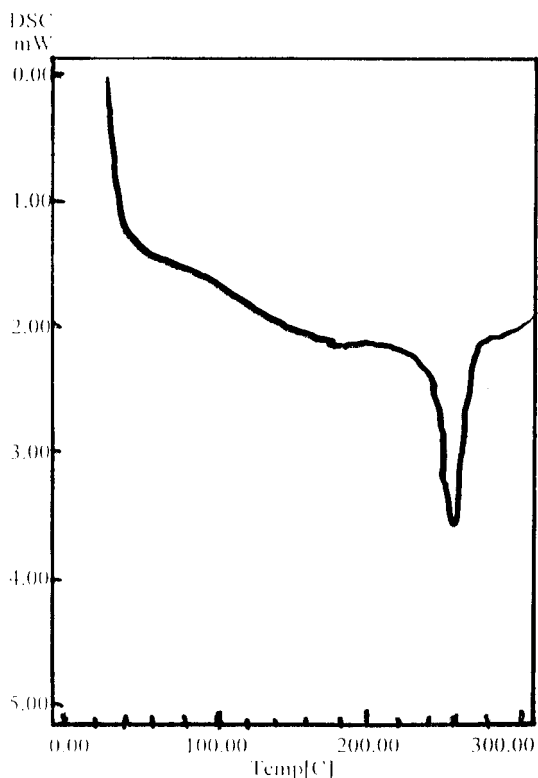


Figure 15 DSC thermogram for PET sample heated at a rate of 10°C/min.

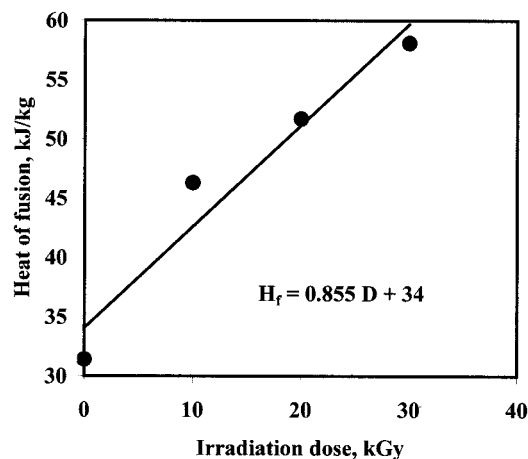


Figure 16 Dependency of the heat of fusion on irradiation dose.

Equation (23) shows that the heat of fusion increases at a rate of 0.855 kJ/kg with the increase in dose with 1 kGy. A value of 34.05 kJ/kg is given for the heat of fusion for unirradiated PET fabric.

X-ray diffraction analysis

The effect of radiation dose on the structure of unirradiated PET fabric is shown in Figure 17, which shows four principal peaks for unirradiated and irradiated PET samples located at 2θ values of 14, 17, 23, and 26°. The main peak for unirradiated PET fabric is at $2\theta = 14^\circ$ and lattice spacing (d) of 6.2506 Å, with a maximum intensity of 60 counts per second (cps). The peak broadens with an increase in dose and the intensity decreases slightly to 58 cps at 10 kGy dose. A further increase in dose results in a decrease in inten-

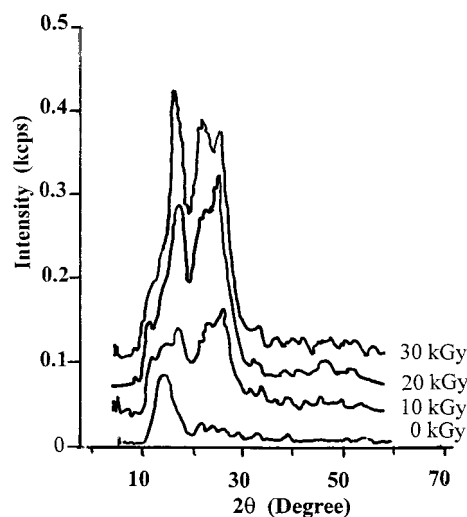


Figure 17 X-ray diffraction pattern for PET samples irradiated to doses of 0, 10, 20, and 30 kGy.

sity from 37 to 30 cps as the dose increases from 20 to 30 kGy. The intensities given in Figure 17 are the net values, given that the background intensity is subtracted from the results.

Irradiating PET fabric to different doses resulted in the formation of new peaks at 2θ values of 17, 23, and 26°. The peak parameters given in Table V for unirradiated and irradiated samples are the angle (2θ) in degrees, the lattice spacing (d) in angstroms (Å), and the peak intensity in cps. The percentage relative intensity (%RI) was also calculated. Table V shows that the peak intensity at 2θ values of 17, 23, and 26°, corresponding to lattice spacings of 5.6969, 3.8102, and 3.4182 Å, respectively, increases with the increase in dose. Figure 18 shows a linear increase in peak intensity with increase in dose up to 20 kGy and deviation from linearity is observed for the peaks at 23 and 26° as the dose increases to 30 kGy. The linearity of the peak at $2\theta = 17^\circ$ is extended up to 130 cps intensity for the 30 kGy dose.

The relative intensity of the peaks characterizing irradiated samples is dependent on peak parameters (2θ and d) and radiation dose (Table V). The RI of the peak at $2\theta = 26^\circ$, and $d = 3.4182$ Å is 100% at 10 and 20 kGy doses. A further increase in dose to 30 kGy shifted the maximum RI to the peak at $2\theta = 17^\circ$ and $d = 5.6969$ Å. The increase in peak intensity of the peak at 17° from 109 to 130 cps at 30 kGy dose is at the expense of the decrease in the intensity of the 26° peak from 130 to 99 cps (Table V).

The results shown in Table V and Figure 18 indicate significant changes in the structure of PET fabric attributed to the increase in radiation dose. The formation of new radiation-induced peaks, the disappearance of the $2\theta = 14^\circ$ peak characterizing unirradiated fabric, and the growth in peak intensities with increase in radiation dose should be explained by the interaction of gamma rays with PET fiber. It is well known that irradiation results in the scission of polymer molecules with random chain scission, most probably at the ester linkage of PET fiber. This causes a decrease in the polymeric molecular weight and changes in the degree of crystallinity of PET. The decrease in chain length or increase in polymer segments resulting from radiation increases the freedom of the crystallites to

TABLE V
X-ray Diffraction Parameters for Unirradiated and Irradiated PET Fabric

| Peak | 2θ (°) | d (Å) | Intensity (cps) | | | |
|------|---------------|---------|-----------------|--------|--------|--------|
| | | | 0 kGy | 10 kGy | 20 kGy | 30 kGy |
| 1 | 14 | 6.2506 | 60 | 58 | 37 | 30 |
| 2 | 17 | 5.6969 | 0 | 59 | 109 | 130 |
| 3 | 23 | 3.8102 | 0 | 65 | 118 | 126 |
| 4 | 26 | 3.4182 | 0 | 75 | 130 | 99 |

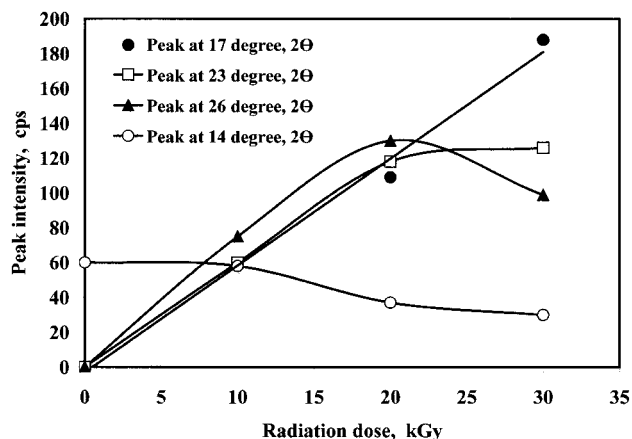


Figure 18 Dependency of peak intensity, at 2θ values of 14, 17, 23, and 26°, on radiation dose.

rotate about certain axes, such that the free energy of the system tends to a minimum. Parallel planes with d spacings of 3.4182 Å will be aligned such that the conditions to meet Bragg's law are fulfilled. An increase in dose to 20 kGy increases the number of scissions and consequently increases the number of planes with spacing of 3.4182 Å, resulting in an increase in peak intensity. As the dose increases to 30 kGy the planes with spacing of 5.6969 Å change their positions and align to fulfill maximum diffraction intensity. Planes of $d = 3.4182$ Å deviate from maximum fulfillment of diffraction conditions. Again, the system free energy decreases at such a radiation dose.

The increase in the number of scissions by dose increase tends to decrease the free energy of the system by increasing its entropy by the increase in the degree of disorder. Consequently, the apparent activation energy of thermal degradation of PET fabric should decrease by an amount proportional to the absorbed energy resulting from radiation. Thus, the apparent activation energy of irradiated fiber $Q_{irr} = (Q_{unirr} - \Delta E_{abs})$. This explains the decrease in the apparent activation energy with the increase in absorbed dose (Fig. 10).

CONCLUSIONS

The following conclusions were reached from the study of the kinetics of the second stage of the degradation process for PET samples irradiated to doses of 10, 20, and 30 kGy:

1. The degradation process follows a second-order kinetics and is independent of radiation dose or heating rate.
2. The reaction rate constant (k_c) is dependent on the radiation dose and heating rate and its value is in the order of magnitude of 10^{-4} and 10^{-3}

s^{-1} for the heating rates of 5 and 30°C/min, respectively.

3. The apparent activation energy (Q) and the logarithm of the preexponential rate constant ($\log A$) decrease linearly with the increase in dose (D) at rates of 3.32 kJ mol⁻¹ kGy⁻¹ and 0.177 s⁻¹ kGy⁻¹ with intercepts of 249 kJ/mol and 12.26 s⁻¹, respectively, for Q and $\log A$ of unirradiated fabric.
4. A direct relationship is established between the percentage decrease in Q and $\log A$ and the percentage decrease in the temperature corresponding to 50% conversion ($T_{50\%}$). A decrease in $T_{50\%}$ by 1% results in a decrease in Q and $\log A$ by 1.855 and 2.1%, respectively.
5. Changes in Q and $\log A$, resulting from radiation, mechanical and thermal treatments, or their combinations can be predicted from the shift in $T_{50\%}$. This emphasizes the importance of the history of the fibers on the thermal properties.
6. DSC and XRD studies revealed changes in the fabric crystallinity attributed to irradiation. DSC measurements show a linear increase in the heat of fusion with an increase in dose at a rate of 0.855 kJ kg⁻¹ kGy⁻¹. XRD analysis confirmed structural changes, arrangement, and/or formation of compact crystal lattice with patterns deviating from those of unirradiated fiber.

References

1. Frohlich, F. W. *Int Fiber J* 1997, 12, 3.
2. Harris, W. B. *Int Fiber J* 1996, 11, 5.
3. El-Gendy, E. H. *Indian J Fibre Text Res*, accepted.
4. El-Gendy, E. H. Personal communication.
5. Stannett, V.; Walsh, W. K.; Bittencourt, E.; Liepins, R.; Surles, J. R. *J Appl Polym Sci* 1977, 31, 201.
6. Liepins, R.; Surles, J. R.; Morosoff, N.; Stannett, V. T.; Barker, R. H. *Radiat Phys Chem* 1977, 9, 465.
7. Zahran, A. H.; Stannett, V.; Liepins, R.; Morosoff, N. *Radiat Phys Chem* 1980, 16, 265.
8. Choi, T. H.; Lee, J. K.; Kong, Y. K.; Chang, H. S. INIS KAERI396RR12980, International Nuclear Information System of the International Atomic Energy Agency, Vienna, Austria, 1980.
9. Kong, Y. K.; Chang, H. S.; Lee, J. K.; Choi, J. H. *J Korean Nucl Soc* 1980, 12, 1.
10. Kaji, R.; Neyagawe, O.; Onkuna, H.; Okada, J. *ISSSB 0034-9875*, 1979.
11. Nor, H. M. INIS PPAT47, International Nuclear Information System of the International Atomic Energy Agency, Vienna, Austria, 1986.
12. Sundardi, F.; Kadariah, X.; Marlianti, I. *J Appl Polym Sci* 1983, 28, 3123.
13. Ozawa, T. *Bull Chem Soc Jpn* 1965, 38, 1881.
14. Nishizaki, H.; Yoshida, K.; Wang, J. H. *J Appl Polym Sci* 1980, 25, 12.
15. Wen, W. Y.; Lin, J. W. *J Appl Polym Sci* 1978, 22, 8.
16. Friedman, H. L. *J Polym Sci Part C* 1963, 6, 183.
17. Freeman, E. S.; Carroll, B. *J Phys Chem* 1958, 62, 394.
18. Chatterjee, P. K.; Conrad, C. M. *J Polym Sci Part A-1* 1968, 6, 3217.
19. Cooney, J. D.; Day, M.; Wiles, D. M. In *Proceedings of the 7th International Conference on Thermal Analysis*, 1982; Vol. 2, p 1325.
20. Gooding, E. P. *Soc Chem Ind* 1961, Monograph 13, 146.
21. Birdlodeanu, C.; Vasile, C.; Schneider, I. A. *Makromol Chem* 1976, 177, 121.
22. Hedges, J. H.; Baer, A. D.; Ryan, N. W. In *Proceedings of the Seventeenth International Symposium on Combustion*, The Combustion Institute, Pittsburgh, PA, 1978; p 1173.
23. Matusevich, Y. I.; Kumachev, A. I. *Tezisy Dokl Resp Konf Molodykh Uch-Khim* 1977, 1, 70.
24. Bechev, Kh.; Lazarova, R.; Dimova, L.; Dimov, K. *Khim Ind (Sofia)* 1980, 8, 341.
25. Kissinger, H. E. *Anal Chem* 1957, 21, 1702.
26. Horowitz, H. H.; Metzger, G. *Anal Chem* 1963, 35, 1464.
27. Coats, A. W.; Redfern, G. B. *Nature* 1964, 201, 68.